Applications of Twisted Hollow Waveguides as Accelerating Structures

Joshua L. Wilson, *Student Member, IEEE*, Aly E. Fathy, *Fellow, IEEE*, Yoon W. Kang, *Senior Member, IEEE*, and Cheng Wang

***Abstract*—A new class of accelerating structures employing a uniformly twisted waveguide is considered. Such a twisted helical structure can be designed to have a specified longitudinal cross section. The design of twisted accelerating structures is discussed with regard to particle velocity and strength of the accelerating field. It is shown how to choose a cross section and twist rate in order to produce a slow wave with a given velocity. With two representative structures, obtained wave velocities range from the speed of light, c, down to 61% the speed of light, while R/Q values of over 1,000 Ω/m have been achieved. A novel two dimensional finite difference based solver is employed to analyze the twisted structures considered. Two twisted cavity prototypes are fabricated and measured, and good agreement is obtained between measured and predicted dispersion curves.**

***Index Terms*—Accelerator cavities, slow wave structures, traveling wave tubes.**

I. Introduction

ACCELERATING structures exploit the interaction of an electromagnetic wave with a charged particle to increase the kinetic energy of the particle. In order to accomplish this, the velocity of the wave must be matched to that of the particle. This precludes the use of any simple hollow waveguide structure, as these all support waves that travel faster than c.

The problem of slowing the phase velocity of an electromagnetic wave to c or below has been a topic of extensive investigation. The standard approach to slowing the EM wave has been to introduce periodic reactive loading to the hollow waveguide or cavity. This can be done by using periodically spaced irises as in the conventional disk-loaded accelerating structure (see [1] for a typical design) or by using some smoothly corrugated guide as in the elliptical TESLA-type cavity [2]. Whatever the nature of the reactive loading, the result can be a slow-wave periodic structure whose phase velocity is matched to the particle. However, the non-uniform cross section of these cavities gives rise to troubling trapped modes which can cause beam instabilities, fields whose magnitudes vary significantly along the axis, and added manufacturing costs.

There have also been efforts to develop slow wave structures which do not employ corrugation. For example, a simple method that has been thoroughly investigated involves using a TM mode in a waveguide partially loaded with dielectric material [3]–[5]. Dielectric loaded accelerating structures show great promise in damping of higher order modes (HOMs) [3], yet the presence of the dielectric presents challenges in areas of manufacturing cost and vacuum conditioning. Also, application of dielectric loaded cavities to superconducting accelerators is not practical.

Here, we discuss the accelerator application of a uniformly twisted hollow waveguide and compare with conventional accelerating cavities. Because the uniformly twisted guide is geometrically self-similar along a continuous helical path, it deserves consideration as a special class of periodic structure and possesses unique features making it an interesting candidate for accelerating structures.

The idea of a twisted waveguide accelerating structure was proposed in a previous paper [6]. In that paper, it was shown that a twisted waveguide could support electromagnetic waves that traveled with a phase velocity less than c. Since this type of structure has a uniform cross section, it can possibly be fabricated without welding or brazing unlike reactively loaded accelerating structures. In [6], MAFIA code was used to simulate the twisted waveguide using stacked waveguide slices. In this paper, we extend the analysis of the twisted waveguides using a specially designed two-dimensional simulation method [7]. Although ordinary EM codes (such as MAFIA) can yield accurate results, the custom code we have developed specifically for twisted guides can run much faster and facilitate easier optimizations.

An important design consideration is the optimization of the shunt impedance R, defined as

$$R = \frac{V^2}{2P}, \tag{1}$$

where V is the on-axis accelerating potential and P is the dissipated power. Because this parameter is dependent on the material of the cavity walls, the shunt impedance is often normalized to the quality factor Q. Thus, the value of R/Q is an important figure of merit for a cavity geometry. Often, when dealing with waveguides or long cavities, R/Q is normalized to the length, making R/Ql a useful figure of merit if l is the cavity length.

In this paper, we discuss the helical geometry specifically as it compares to ordinary rotationally symmetric accelerating structures. Then, the electromagnetic modes of twisted structures

Manuscript received October 20, 2008; revised February 25, 2009. Current version published June 17, 2009. This work was supported by ORNL-SNS. The Spallation Neutron Source is managed by UT-Battelle, LLC, under contract DE-AC05-00OR22725 for the U.S. Department of Energy.

J. L. Wilson and A. E. Fathy are with the Department of Electrical Engineering and Computer Science, University of Tennessee, Knoxville, TN 37916 USA (e-mail: jwilso75@utk.edu).

Y. W. Kang is with the Oak Ridge National Laboratory, Oak Ridge, TN 37831 USA.

C. Wang is with the University of Massachusetts, Amherst, MA 01003 USA.

Color versions of one or more of the figures in this paper are available online at http://ieeexplore.ieee.org.

Digital Object Identifier 10.1109/TNS.2009.2017534

are analyzed and discussed. Prototypes of twisted accelerating structures are presented, and experimental results are compared to theory. The dispersion characteristics of twisted guides are discussed with relation to conventional periodically loaded accelerating structures. Finally, we present some practical design considerations for twisted accelerating guides.

II. Twisted Geometry

The mathematical definition of a twisted volume was given in a previous paper [7], where we utilized the twisted (or helicoidal) coordinate transform employed by Lewin [8].

$$\begin{aligned} x' &= x\cos pz + y\sin pz \\ y' &= y\cos pz - x\sin pz \\ z' &= z. \end{aligned} \tag{2}$$

Here, p is some constant twist rate. We consider that a twisted structure can be designed to have any desired longitudinal cross section by appropriately selecting a transverse cross section to be twisted. Thus, all the well-known accelerator geometries (iris-loaded, elliptical, etc.) have twisted analogs whose longitudinal cross section is identical.

Such a twisted analog can be constructed in the following fashion. Assume we have a rotationally symmetric structure defined in cylindrical coordinates (ρ, ϕ, z) by

$$\rho < g(z), \tag{3}$$

where g is some periodic function with periodicity Δz. We define a 2D transverse cross section

$$\rho(x,y) < g\left(\frac{\phi(x,y)\Delta z}{\pi}\right) \tag{4}$$

and set the twist rate

$$p = \frac{\pi}{\Delta z}. \tag{5}$$

When $\phi(x,y)$ varies in range from 0 to 2π, the argument of g varies from 0 to $2\Delta z$. The reason for including two cycles of the periodic structure in the 2D cross section is to ensure that the resulting cross section has symmetry about the origin. (This symmetry is necessary to ensure that the field components at the center of the twisted guide are purely axial.) Once the cross section has been obtained, the transformation of (2) is then used to generate the analog. The twisted analog also allows some interesting comparisons to be made between twisted and rotationally symmetric non-twisted structures, as both can be used as slow wave structures.

The twisted analog defined above is not unique. It is easily observed that any two dimensional profile defined by

$$\rho(x,y) < g\left(\frac{m\phi(x,y)\Delta z}{2\pi}\right) \tag{6}$$

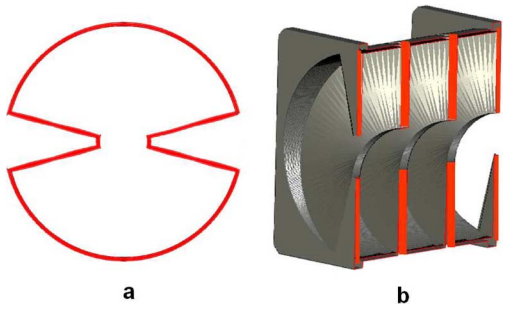

Fig. 1. A twisted analog to the disk-loaded slow-wave structure.

and twist rate

$$p = \frac{2\pi}{m\Delta z} \tag{7}$$

has identical longitudinal cross section to the original rotationally symmetric structure for any even integer m. An example of such a twisted analog is shown in Fig. 1. In this case, the "keyhole" cross section of (a) is extruded along a twisted path to form the volume (b), whose longitudinal cross section is identical to a disk-loaded accelerating structure.

In this study, two twisted structures are compared to their rotationally symmetric analogs. The first is the "keyhole" structure just described, and the second is an analog to the elliptical TESLA-style cavity, specifically related to the medium beta superconducting cavity at the Spallation Neutron Source (SNS) [9].

III. Electromagnetic Modes in Twisted Waveguides

In general, modes in twisted guides are hybrid in nature, being neither strictly TE or TM. However, our current investigations reveal that the modes tend to take on characteristics of either quasi-TE modes which have a very small z-directed electric field, or quasi-TM modes with a relatively strong E_z component. Twisted guides can support both standing and traveling waves modes. In this paper, our analysis is mostly concerned with traveling wave modes. Standing wave solutions can be constructed simply from the traveling wave modes by superposing two counter propagating traveling wave modes.

Because the twisted waveguides under consideration are periodic in z, Floquet's theorem predicts that the fields will also have the same periodicity, except for a multiplicative phase factor. In this case, the period of the twisted waveguide will be $2\pi/p$. However, for the case of a uniformly twisted waveguide, it turns out that one can make an even stronger statement.

Assume the fields at some $z = z_0$ are known. Moving a distance dz along the axis of the twisted structure, the structure is exactly the same except for some rotation of angle $p\,dz$. Therefore, as shown in [10] for structures having "screw symmetry", the fields intuitively should be the same except for a phase factor. This relation holds true for any dz, not just $dz = 2\pi/p$. In particular, we can send dz to zero and discover that for an infinite twisted waveguide, the variation of the fields along the axis of propagation involves only simple phase variation. In

other words, except for the constant rotation of the fields, the z dependence can be factored out as $e^{-j\beta z}$ for some phase constant β. In terms of the twisted coordinates,

$$\boldsymbol{E}(x', y', z') = \boldsymbol{E_0}(x', y')e^{-j\beta z'}. \tag{8}$$

This separation of the z dependence for twisted guides is significant, since it cannot generally be done for periodic structures. In (8), it was possible to replace $e^{-j\beta z}$ with $e^{-j\beta z'}$, since z and z' are numerically equal. Similar relations hold for $\boldsymbol{H}$. Thus, if a twisted coordinate system is used, the fields in a twisted waveguide can be represented in exactly the same fashion as for an infinite straight waveguide. A more mathematical way of showing this equivalence between straight and twisted fields involves an equivalent straight waveguide loaded with some anisotropic material. This equivalent was given approximately in [6], and an exact equivalent is given in [7], [11]. The anisotropic material equivalent also shows that one can make a twisted structure effectively "look" like a dielectric loaded structure without having the undesirable effects associated with real dielectrics.

In addition to simplifying the analysis greatly, this property of the uniformity of the fields along the axis of propagation also provides practical advantages for accelerating structures. In a periodic structure, the fields can be expressed by an infinite Floquet expansion. For example,

$$\boldsymbol{E} = \sum_{n=-\infty}^{\infty} \boldsymbol{E}_n(x, y)e^{j\beta_n z} \tag{9}$$

where

$$\beta_n = \beta_0 + \frac{2\pi n}{\Delta z}. \tag{10}$$

However, in the twisted coordinate system of (2), we have $\boldsymbol{E}_n = 0$ for all $n \neq 0$, due to the fact that the waveguide becomes equivalent to a straight waveguide under the coordinate transformation. Thus, only a single space harmonic is present. In conventional coordinates (cylindrical or cartesian), an infinite number of space harmonics will still be needed, but along the z axis (which coincides with the z axis of the twisted coordinate transform) all higher space harmonics must vanish:

$$\boldsymbol{E}_n(x = 0, y = 0) = 0, \quad n \neq 0. \tag{11}$$

The implication of this is that along the axis of an infinite twisted structure there is no variation in the magnitude of the fields—only in the phase. This distinguishes the twisted guide from conventional slow-wave structures (like corrugated or iris-loaded waveguides). Since only the $\boldsymbol{E}_0$ harmonic travels synchronously with the particle beam and acts cumulatively to accelerate the particles, the elimination of other harmonics is very desirable, and it could be accomplished using the twisted structure. Another important aspect of the twisted guides we are considering is the fact that modes can be constructed such that the on-axis fields are purely axial, *i.e.*, the only field components present at the center of the guide are E_z and H_z.

TABLE I
PARAMETERS FOR TWISTED ANALOG TO DISK-LOADED ACCELERATING CAVITY

Parameter	Value	Unit
Outer radius	5.493	cm
Inner radius	1.135	cm
Twist Rate	89.76	Radians/m
Phase advance per $\frac{1}{2}$ turn	$\frac{2\pi}{3}$	Radians
Notch angle	30	Degrees
$\frac{R}{Ql}$	716	Ω /m

This is due to the fact that we have restricted ourselves to twisted structures that are invariant to a 180 degree rotation about the center axis. However, particles traveling off axis may experience slight non-axial fields, and further investigation is needed to determine whether narrow-band coupling devices may cause problems for beams traveling slightly off axis.

To demonstrate the slow-wave capabilities of twisted structures, we again consider the shape of Fig. 1. To design a practical accelerating structure having this geometry, we started out with the dimensions of the well-known SLAC accelerating cavity [1]. It was found, however, that the twisted analog had phase velocity greater than c. To lower the phase velocity, the outer diameter of the cavity was increased from 4.13 cm to 5.49 cm until the velocity was c. A similar increase in outer diameter was necessary for each type of twisted analog we studied to keep the phase velocity the same. (A detailed sensitivity analysis of the structure to variations in cross-sectional dimensions is currently under investigation.) The physical parameters of this structure are given in Table I. The accelerating parameters of this structure in terms of R/Q and dispersion characteristics are discussed in detail in later sections.

The notch angle referred to in Table I is the angle of the notch in the "keyhole" transverse cross section. This example shows how a twisted structure can easily be compared to a non-twisted rotationally symmetric structure. For example, in the SLAC accelerating cavity, the phase advance per cell is $2\pi/3$. Similarly, one can consider one half twist of the twisted waveguide as a "cell" and define a $2\pi/3$ mode in the same way. However, it should be noted that this assumption is simply for comparison, since the phase advance determined for the corrugated structure can not be related directly to the twisted structure.

A visual representation of the fields in such a structure is provided using CST Microwave Studio simulation [12], and is shown in Fig. 2. A periodic boundary condition was established at the ends of the twisted structure. The Microwave Studio solution represents a standing wave rather than a traveling wave solution. Such a solution can be easily constructed from two counter-propagating traveling wave solutions. The vector electric field is shown as arrows in the figure. The z component of the electric field is plotted in Fig. 3 for a particle on the z-axis, a particle 0.6 cm off axis, and a particle 0.9 cm off axis. Very far from the center of the guide near the groove region, it is easily seen that the field does not vary sinusoidally with the longitudinal coordinate z, indicating that many space harmonics are present in this region. On the other hand, close to the center of the guide, the field variation is sinusoidal as all space harmonics except the fundamental disappear.

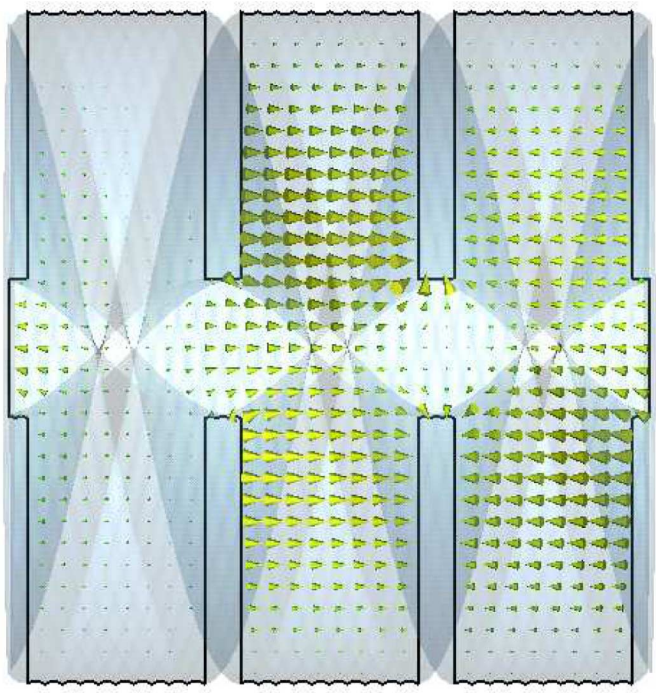

Fig. 2. Electric field of twisted analog of a disk-loaded cavity: CST simulation.

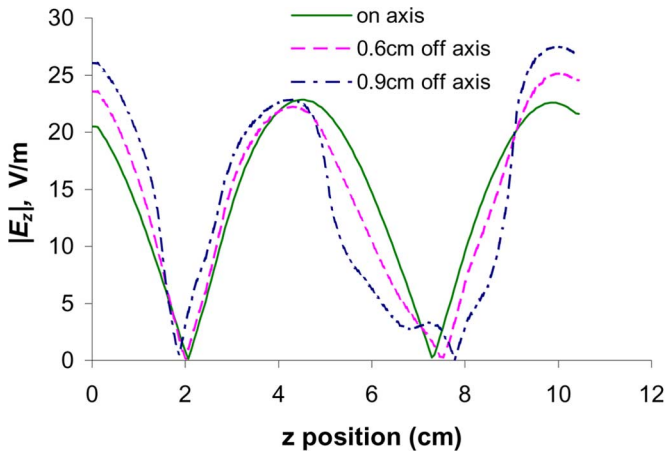

Fig. 3. Magnitude of $\boldsymbol{E_z}$ for on-axis and off-axis particles: CST simulation.

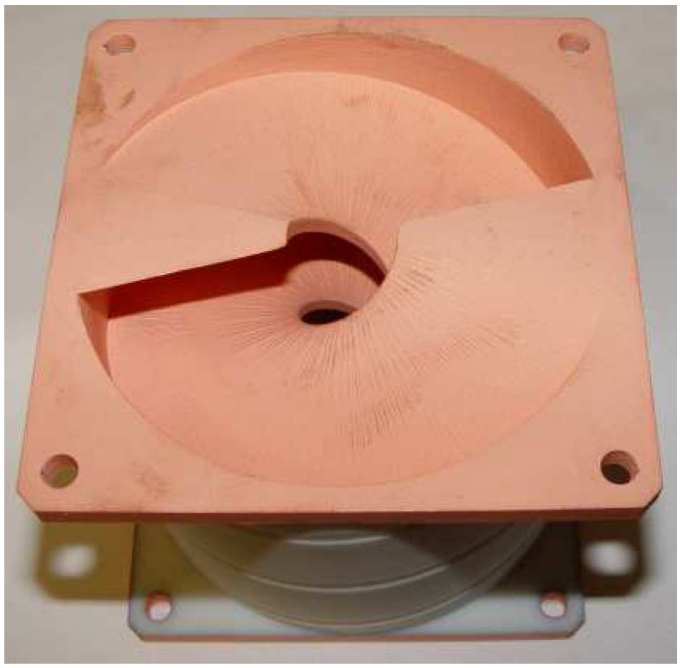

Fig. 4. Fabricated "keyhole" cross-section prototype.

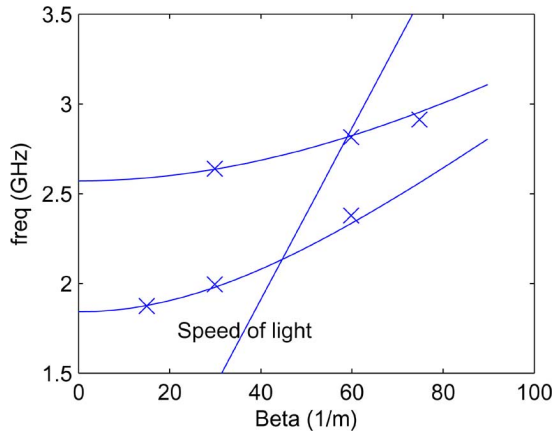

Fig. 5. Predicted and measured dispersion curves for two modes of a twisted analog to a disk-loaded cavity. The mode with higher frequency is the quasi-TM accelerating mode; the lower frequency mode is a quasi-TE mode. The x's are experimental points.

IV. Experimental Investigation

A twisted cavity prototype for the "keyhole" structure with the dimensions in Table I was printed using an SLA (Stereolithography Apparatus) process. In this process, a resin base structure is formed by 3D printing with 5 mil layers. The entire process has a tolerance of 10 to 20 mils. The inside surface was then electroplated with copper. The prototype is shown in Fig. 4. Two identical prototypes were made and placed end to end for a total of three complete twists. The structures were terminated with copper shorting plates to form a cavity resonator. The twisted cavity supports standing wave modes which can be measured and compared to theoretical predictions. A small probe was inserted through each shorting plate, and the transmission was measured to determine the cavity resonances. A bead pull measurement was also performed to determine the value of the phase constant for each of the resonances. The theory of the bead pull technique is discussed in [13]–[15]. This measurement allowed us to determine the variation of the electric field along the cavity axis, from which the phase constant could easily be extracted. Knowing the resonant frequency and the phase constant for each resonant mode, it is now possible to compare the dispersion characteristics to those predicted by theory [7]. The comparison is shown in Fig. 5. The higher frequency mode is the quasi-TM mode of interest, while the lower frequency mode is a quasi-TE mode with very low R/Q. The straight line is for $v_p = c$, which represents the boundary between fast and slow waves. There is generally good agreement between the experimental and theoretical results. The discrepancies are likely caused by disturbances introduced by the end walls, which perturb the cavity fields from what they would otherwise be in an infinite twisted guide.

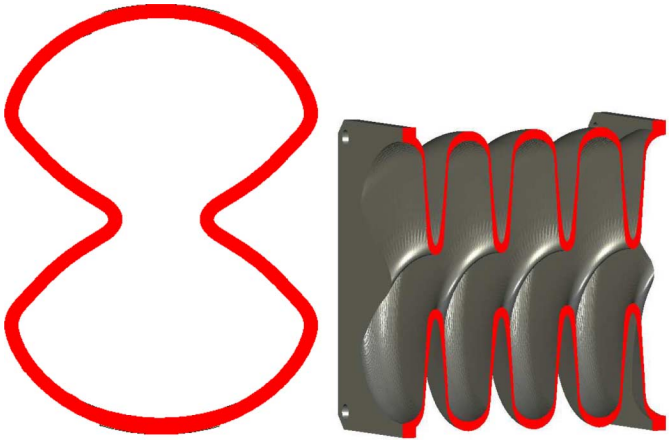

Fig. 6. Cross section and cutaway view of the twisted elliptical prototype.

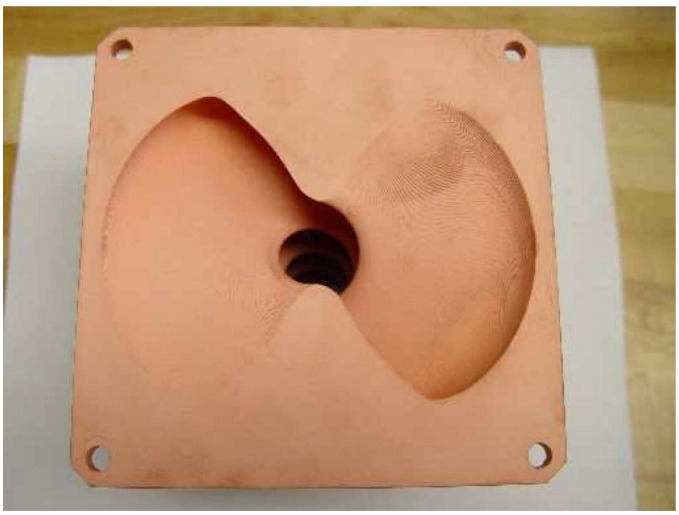

Fig. 7. Fabricated elliptical cross-section prototype.

A twisted analog to an elliptical (TESLA-style) cavity is also considered. This design was accomplished in the same way as the disk-loaded analog design, by using (4)–(5). It was found necessary to increase the outer radius in order to ensure that the relativistic $\beta = (v/c) = 0.61$, which is the same as the SNS medium-beta superconducting cavity. (Note that this β is different from the phase constant discussed earlier.) The final prototype design had inner radius 1.24 cm, outer radius 6.37 cm, and twist rate 96.2 Rad/m. Fig. 6 shows the "dumbbell" shape of the transverse cross section of this slow wave structure, and a cutaway view showing the longitudinal cross section, which is identical to the well-known TESLA-type elliptical profile. Again, two identical prototypes were fabricated, and when placed end to end provide four complete twists. The prototype is shown in Fig. 7, and the dispersion curve for the accelerating mode is shown in Fig. 8. Many additional resonances were observed other than the ones shown in Fig. 8, but their relatively low Q values afforded by the rough cavity walls and other experimental factors prohibited an accurate bead pull measurement of these modes. However, the data points gathered for the accelerating mode of interest show good agreement with theory.

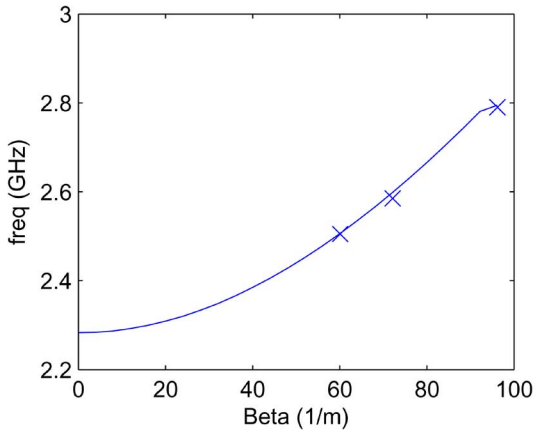

Fig. 8. Predicted and measured dispersion curves for the accelerating mode of an elliptical twisted guide. The x's are experimental points.

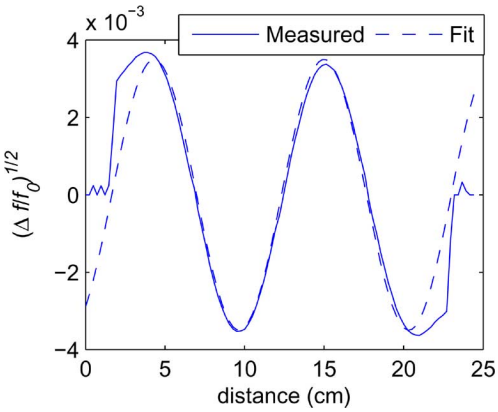

Fig. 9. Measured field in the twisted analog of the disk-loaded cavity.

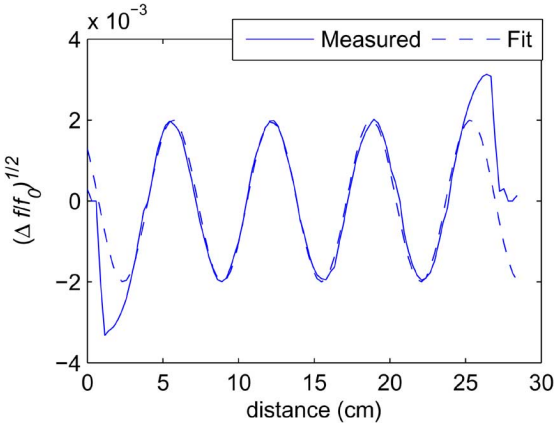

Fig. 10. Measured field in the twisted elliptical cavity.

In addition to the dispersion characteristics, the profile of the electric field gathered from the bead pull measurement was analyzed, and experimental R/Q values for each of the two prototypes were obtained. The z component of the axial electric field is proportional to the square root of the change in resonant frequency due to the bead at each position. These measurements are shown for the twisted analog to the disk-loaded and elliptical cavities in Figs. 9 and 10, respectively.

TABLE II
COMPARISON OF MEASURED AND PREDICTED R/Q VALUES FOR TWO TWISTED PROTOTYPES

Cavity type	Measured $\frac{R}{Ql}$	Predicted (Infinite Structure) $\frac{R}{Ql}$
Disk-loaded	776 Ω/m	716 Ω/m
Elliptical	248 Ω/m	223 Ω/m

The appearance of the electric field along the cavity axis is seen to be roughly sinusoidal in the center of the cavity. Since theory predicts the existence of only one space harmonic along the center axis, and hence a simple sinusoidal variation of the electric field, a sinusoidal curve was designed to fit the measured data and is shown alongside the data in Figs. 9 and 10. The sinusoid has distribution

$$y = A\sin(kz + \phi), \tag{12}$$

where

$$k = \frac{\omega}{\beta c}. \tag{13}$$

Here, β is the relativistic quantity that is equal to 1 for the twisted analog of the disk-loaded cavity and 0.61 for that of the elliptical cavity. The other constants, A and ϕ, are chosen to best fit the measured data. These data show that the electric field has a sinusoidal appearance close to the center of the cavity, while end effects cause a deviation close to the cavity end walls.

Using the techniques of [15], the standing wave R/Q values of the twisted structures were found. While the measured R/Q was for a standing wave pattern, in the simulation we assumed a traveling wave. However, if a standing wave mode is considered a sum of two traveling wave modes, it is obvious that only the forward traveling wave (traveling synchronously with the particle) contributes to the acceleration, and thus to the value of V_{acc}. Yet, the energy of the wave will reflect both the forward and backward components. As a result, the traveling wave R/Ql is twice the standing wave value. Thus, to calculate the traveling wave R/Ql, the measured R/Q was multiplied by 2 and taken over the length of the cavity.

Table II shows a comparison between measured and predicted traveling wave R/Ql values. There are several sources of measurement error. The formulas given in [15] are only valid if all other field components except E_z are zero, which may not be exactly the case for the measured twisted structures. Temperature drift during the measurement and uncertainty regarding the precise value of the form factor for the perturbing metal bead also contributed some error. In addition, end effects may play a role, causing an increase of the field strength close to the metal end walls of the cavity. This would cause the measured R/Ql to be more than what would be predicted assuming the cavity was infinite in length, explaining why the measured R/Ql values to be higher than predicted for an infinite structure. This is particularly the case with the elliptical structure, where edge effects are seen from Fig. 10 to be quite pronounced.

The problem of reducing end effects requires careful consideration. Although not addressed in detail here, we have shown previously that in some cases the end effects can be mitigated by introducing a curved boundary surface as the end wall [6]. Another approach is to eliminate the end walls and leave them open to a waveguide interface, which then has to be properly matched to the twisted structure. These considerations are beyond the scope of the present paper.

We have considered the twisted structure in terms of R/Q since this accelerating parameter is geometry dependent only, not material dependent. Also, R/Q is very easy to determine using the 2D simulation method we have used. A future investigation may be made into values of shunt impedance for a number of different materials, both superconducting and normal conducting, since the shunt impedance ultimately determines the beam energy gain at a given amount of rf input.

V. DISCUSSION OF DISPERSION CHARACTERISTICS

In this section, we will discuss two desirable features of the dispersion characteristics that are unique to twisted guides. First, we would show that the dispersion characteristics are particularly desirable in the prevention of certain types of higher order trapped modes. Second, we demonstrate that the problem of mode separation can be dealt with more easily than in non-twisted periodic geometries. There are several mechanisms which can lead to trapping of higher order modes in accelerating cavities. One is the frequency difference between the end cells and inner cells caused by improper RF matching of the end cells. These types of trapped modes are not the subject of our discussion here. However, higher order trapped modes can also appear in accelerating structures of infinite extent (independent of the influence of boundary cells) because of stop-bands in the dispersion characteristics. When beam energy is deposited in such a stop band, the excited fields are evanescent and cannot propagate out of the structure to higher-order mode dampers. Such modes are particularly problematic in superconducting cavities, because the large Q values allow these unwanted resonances to continue for a long time before finally decaying due to wall losses. In the case of the twisted guide, however, there are no stop bands above the cutoff frequency of the fundamental propagating mode. Although this may not be apparent from the appearance of Figs. 5 and 8, these figures show only the first branch of the propagating modes (*i.e.,* those whose phase constant is between 0 and $\pi/\Delta z$). In reality, these modes can be thought of to continue on to infinitely high values of β by virtue of the straight waveguide equivalent.

A second observation relates to mode spacing in these accelerating structures. Many standing wave periodically loaded accelerating cavities operate close to π mode, or 180 degrees of phase shift per unit cell. However, near the point on the dispersion curve where $\beta = \pi/\Delta z$, the group velocity (calculated as $d\omega/d\beta$) typically approaches zero. This prohibits effective operation, since nearby unwanted modes would be excited very easily. One solution to eliminate the problem of zero group velocity at π mode is the deliberate creation of confluent pass bands, with the point of confluence judiciously selected as the point of the desired π mode operation [16]. However, this requirement places a significant constraint on the design of the periodic accelerating structure. In the case of the twisted waveguide no such problem exists, as the group velocity remains nonzero for all values of the phase constant β.

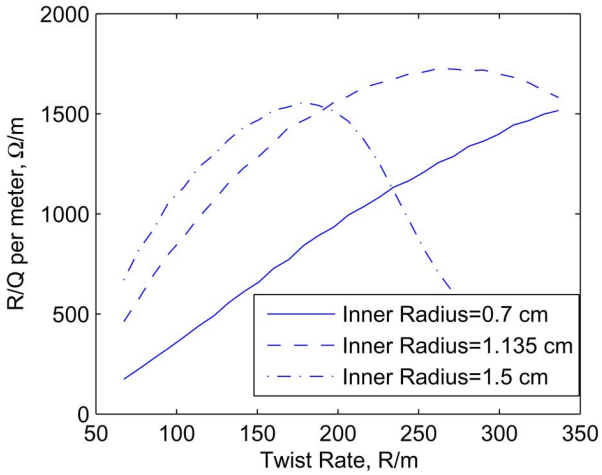

Fig. 11. Simulated effect of changing the inner radius on R/Ql.

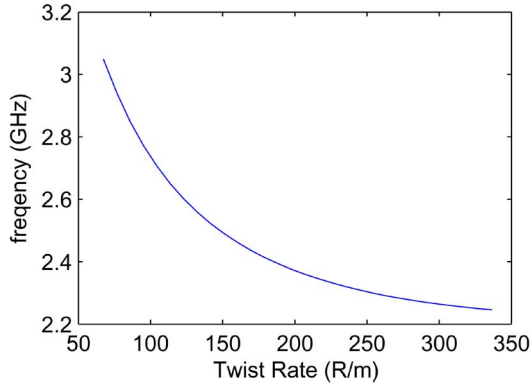

Fig. 12. Simulated frequency as a function of twist rate (phase velocity held equal to c).

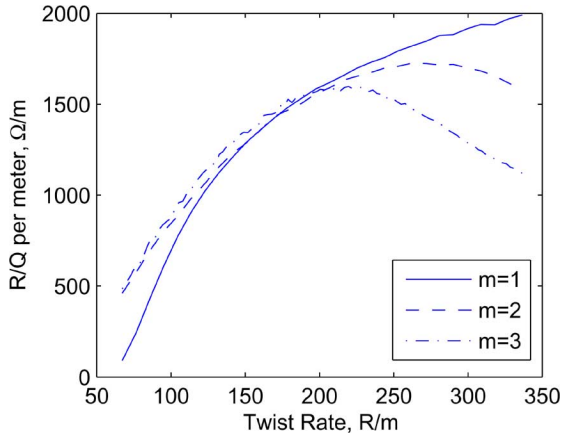

Fig. 13. Simulated effect of changing m on R/Ql.

VI. Design Considerations

In our discussion of practical design consideration, we will consider mainly variations on the twisted analogs to the disk-loaded accelerating structure. While there are infinite number of possible cross sections, this shape can be particularly instructive due to its simplicity. Other cavity shapes, such as the twisted elliptical cavity, can be thought of (at least to first order approximation) as a disk-loaded analog with rounded edges.

We consider the effect of a varying cross section on these curves. Two parameters in particular are varied: the inner radius of the notch (corresponding to the iris radius of the disk loaded analog) and the value of m in (6).

In particular, it was investigated how to maximize the value of R/Q with respect to the rate of twisting for the twisted analog to the disk-loaded accelerating structure. We assumed that the structure was constrained to have a phase velocity equal to c for accelerating relativistic particles. For each value of the twist rate p, the frequency was adjusted in simulation in order to satisfy the phase velocity constraint. This adjustment will be shown later. R/Q was calculated for a traveling wave structure from simulation using the technique found in Appendix I. For the twisted analog to the disk loaded accelerating structure, we show R/Q performance for inner radii of 0.7 cm, 1.135 cm (design value), and 1.5 cm. This is shown as a function of the twist rate in Fig. 11. A clear optimum value of R/Q can be seen, its value and location being functions of the twist rate.

In conventional accelerator cavities, a small iris radius is desirable for higher shunt impedances, but has the drawback that it decreases the maximum allowable size of the beam; so a design tradeoff is often needed. For the experimental prototype, the twist rate was only 89.76 Rad/m, so in practice a relatively higher value for the twist rate will yield higher values of R/Q. Fig. 11 indicates that while the R/Q can be increased somewhat by choosing a smaller inner radius, a larger radius can possibly be desirable at low twist rates, although a higher R/Q can be achieved at higher twist rates with smaller inner radius.

For the design case of 1.135 cm inner radius, the frequency is be adjusted as a function of the twist rate as shown in Fig. 12. This adjustment is necessary in order to maintain the phase velocity at c. In practice, changing the frequency is rather impractical, but a similar adjustment could be affected by scaling all dimensions of the accelerating structure. Such a scaling would (at least to first order) leave both the phase velocity and R/Q unchanged. R/Ql would, in turn, be scaled by the ratio of the new frequency to the original frequency.

We then investigated changing the parameter m in (6). For a given twist rate, changing m leads to either compressing or expanding the longitudinal cross sectional shape in the axial direction. For even values of m, the cross section will be identical to that of a disk loaded cavity. For odd values of m, the cross section would be a "staggered" version of the original cross section. Again, we hold all other parameters constant, and show the effect of changing m on R/Q as a function of the twist rate. We considered values of m ranging from 1 to 3, with $m = 2$ the design value. The results are presented in Fig. 13. In general, the value of m does not effect the R/Q value significantly except at high twist rates. However, higher values of m lead to a more complex structure and may be more difficult to manufacture. Generally, then, lower m values are preferable.

VII. Conclusion

We investigated a new type of accelerating structure consisting of a uniformly twisted waveguide. Using the simple method presented in this paper, it is possible to construct a twisted accelerating structure whose longitudinal cross section matches a predefined shape. Twisted structures have been successfully modeled using a theory presented previously [7], and experimental measurements on two twisted accelerating

$$[g_{ij}] = \begin{bmatrix} x_{x'}^2 + y_{x'}^2 & x_{x'}x_{y'} + y_{x'}y_{y'} & pxy_{x'} - pyx_{x'} \\ x_{x'}x_{y'} + yyx'y_{y'} & x_{y'}^2 + y_{y'}^2 & pxy_{y'} - pyx_{y'} \\ pxy_{x'} - pyx_{x'} & pxy_{y'} - pyx_{y'} & 1 + p^2(x^2 + y^2) \end{bmatrix} \tag{14}$$

$$\begin{aligned} \frac{R}{Q} &= \frac{|E_{z,axis}|^2}{2\omega\left(\frac{U}{l}\right)} \\ \text{or } \frac{R}{Ql} &= \frac{|E_{z,axis}|^2}{2\omega(U)} \\ &= \frac{|E_{3,axis}|^2}{\omega \int\int \left(\sum_{j,k=1}^{3} \epsilon_0 g^{jk} E_j E_k + \mu_0 g^{jk} H_j H_k \right) \sqrt{g} dx' dy'} \end{aligned} \tag{15}$$

cavity candidates indicate excellent agreement with theory in terms of dispersion characteristics.

It has been demonstrated that twisted waveguides are able to slow an electromagnetic wave to velocities below c without the introduction of problematic dielectrics or open structures. These slow wave modes permit interaction with an electron or ion beam. Twisted structures also offer the possibility of HOM free acceleration of on-axis particles because of the vanishing of all higher order space harmonics along the center axis of the guide.

Appendix
Numerical Simulation Details

The twisted accelerating structures were simulated using the two dimensional methods found in [7], specifically the two-dimensional finite-difference frequency domain method. The frequency domain method permits direct extraction of the eigenvectors given a propagation constant β. For each twisted cross section, a two-dimensional structured mesh was generated using the computer code UNAMALLA [17]. We then use the coordinates of the structured mesh to compute the metric tensor components [7]: See equation (14) at the top of the page. At each point in the rectangular $x' - y'$ domain, the physical coordinates x and y are given by the mesh generation program, and the partial derivatives in the equation above can then be approximated using finite differences. For the simulations in this paper, a 51x51 mesh was employed and reasonable convergence was achieved.

The R/Q value can be computed from the simulated traveling wave eigenmode if the energy per unit length U/l is calculated. Then, the following formula is utilized: See equation (15) at the top of the page. Here, E_i and H_i represent the i covariant component of the respective fields in the transformed coordinate system, g^{ij} correspond to the components of the contravariant metric tensor, and g is the determinant of the covariant metric tensor. Equation (15) is valid at the center of the guide, where $E_3 = E_z$. The expression for the total energy per unit length U, which appears in the denominator, is the same whether derived in twisted or Cartesian coordinates. The integration is then performed over the rectangular $x' - y'$ cross section in the transformed coordinate system. The method was analyzed by comparing results to CST for the case of an infinite twisted disk loaded analog of the same type as the measured prototype except with a slightly more rapid twist rate of 150 Rad/m. An agreement to within 6.7% was achieved.

References

[1] R. P. Borghi, A. L. Eldredge, G. A. Loew, and R. B. Neal, *Design and Fabrication of the Accelerating Structure for the Stanford Two-Mile Accelerator*. New York: Academic, 1966, vol. 1.

[2] J. Sekutowicz, "Tesla superconducting accelerating structures," *Meas. Sci. Technol.*, vol. 18, no. 8, pp. 2285–2292, 2007.

[3] C. Jing, W. Gai, J. Power, R. Konecny, S. Gold, W. Liu, and A. Kinhead, "High-power RF tests on x-band dielectric-loaded accelerating structures," *IEEE Trans. Plasma Sci.*, vol. 33, pp. 1155–1160, Aug. 2005.

[4] J. Power, W. Gai, S. Gold, A. Kinkead, R. Konecny, C. Jing, W. Liu, and Z. Yusof, "Observation of multipactor in an alumina-based dielectric-loaded accelerating structure," *Phys. Rev. Lett.*, vol. 92, no. 16, Apr. 2004.

[5] C. Jing, W. Liu, W. Gai, J. Power, and A. Kanareykin, "34.272 GHz multilayered dielectric-loaded accelerating structure," in *Proc. Particle Accelerator Conf.*, 2005, pp. 1952–1954.

[6] Y. W. Kang, "Twisted waveguide accelerating structure," in *Proc. 9th Workshop Advanced Accelerator Concepts*, Aug. 2000.

[7] J. Wilson, C. Wang, A. Fathy, and Y. Kang, "Analysis of rapidly twisted hollow waveguides," *IEEE Trans. Microw. Theory Tech.*, vol. 57, pp. 130–139, Jan. 2009.

[8] L. Lewin, *Theory of Waveguides*. London, U.K.: Newness-Butherworths, 1975.

[9] C. Rode, "The SNS superconducting linac system," in *Proc. Particle Accelerator Conf.*, Jun. 18–22, 2001, vol. 1, pp. 619–623.

[10] P. Crepeau and P. McIsaac, "Consequences of symmetry in periodic structures," *Proc. IEEE*, vol. 52, pp. 33–43, 1964.

[11] D. Shyroki, "Exact equivalent straight waveguide model for bent and twisted waveguides," *IEEE Trans. Microw. Theory Tech.*, vol. 56, pp. 414–419, 2008.

[12] *CST Microwave Studio 2006 User's Manual*. Darmstadt, Germany: CST Ltd.

[13] L. Maier and J. Slater, "Field strength measurements in resonant cavities," *J. Appl. Phys.*, vol. 23, no. 1, pp. 68–77, Jan. 1952.

[14] D. Goldberg and R. Rimmer, "Measurement and identification of HOMS in RF cavities," in *Proc. Particle Accelerator Conf.*, May 12–16, 1997, vol. 3, pp. 3001–3003.

[15] P. Matthews, T. Berenc, F. Schoenfeld, A. Feinerman, Y. Kang, and R. Kustom, "Electromagnetic field measurements on a millimeter wave linear accelerator," *IEEE Trans. Microw. Theory Tech.*, vol. 44, pp. 1401–1409, Aug. 1996.

[16] D. McDiarmid and G. Walker, "Two examples of confluence in periodic slow wave structures," *IEEE Trans. Microw. Theory Tech.*, vol. 16, pp. 2–6, Jan. 1968.

[17] P. Barrera, G. Gonzalez, L. Castellanos, and A. Pérez, Unamalla Mesh Generation Package 2008 [Online]. Available: http://www.mathmoo.unam.mx/unamalla